Materials Research Bulletin 46 (2011) 1192–1196

Contents lists available at ScienceDirect

Materials Research Bulletin

journal homepage: www.elsevier.com/locate/matresbu

Luminescence properties of monoclinic $Cu_4I_4(Piperidine)_4$

Ehsan Jalilian [a,*], Rong-Zhen Liao [b], Fahmi Himo [b], Sven Lidin [c]

[a] Dept. Material and Environmental Chemistry, Arrhenius Laboratory, Stockholm University, SE-106 91 Stockholm, Sweden
[b] Dept. Organic Chemistry, Arrhenius Laboratory, Stockholm University, SE-106 91 Stockholm, Sweden
[c] Dept. Polymer and Materials Chemistry, Lund University, 221 00 Lund, Sweden

ARTICLE INFO

Article history:
Received 12 February 2011
Received in revised form 4 April 2011
Accepted 15 April 2011
Available online 22 April 2011

Keyword:
D. Luminescence

ABSTRACT

A new modification of $Cu_4I_4Pip_4$ has been synthesized under hydrothermal conditions. X-ray crystallography revealed that this compound crystallized in the monoclinic system and consists of a tetrahedral core with composition Cu_4I_4, in which each Cu atom is coordinated by a piperidine molecule via the N atom. In contrast to a previously reported modification of $Cu_4I_4Pip_4$, the present modification shows luminescent properties when exposed to UV-light. In addition, we have used time-dependent density functional theory calculations to characterize both compounds in term of both absorption and emission.

© 2011 Elsevier Ltd. All rights reserved.

1. Introduction

Copper(I)iodides have an interesting and varied structural chemistry due to their flexibility, which is a result of the ability of copper to adopt different geometries [1]. The most severe limitation on the system is given by the tendency for the iodide atoms to form a convex hull within which the Cu atoms are distributed. The complexes are therefore always negatively-charged because of the surplus of iodide. To create neutral clusters, the introduction of soft N/P/S donors has been proven efficient. A complex of particular interest is $Cu_4I_4L_4$ (L = soft N/P/S donor ligands) noted for temperature-dependent luminescence properties. The most well-characterized unit is $Cu_4I_4Pyridine_4$, which emits in the blue part of the spectrum when frozen in toluene at 77 K and in the red part of the spectrum at room temperature in the presence of solvent, while it emits yellow light at room temperature when no solvent is present [2]. The critical parameter that is believed to be the reason for the luminescence properties in Cu(I)–I system is the Cu–Cu distance. In discrete cluster compounds a Cu–Cu distance less than 2.8 Å often signals luminescence, while longer distances tend to be optically dead [3]. There are however notable exceptions to this rule.

One example is given in a report from 1978, where a $Cu_4I_4Pip_4$ cluster with the typically vividly fluorescent tetrahedral Cu_4I_4 core shows no luminescence at all [4]. The reason for this is not fully understood.

In the present paper we wish to report on a new modification of $Cu_4I_4Pip_4$ that, in contrast to the published case, shows the expected luminescence under UV light. We also perform quantum chemical calculations to characterize the absorption and emission properties of the two modifications.

2. Methods

2.1. Synthesis

The formation of the title compound is quite insensitive to molar ratios. We managed to synthesize this compound within a wide range of starting compositions with respect to the Cu:CuO ratio. The best quality crystals we achieved were produced using the molar ratio reported below.

Cu powder (6.09 mmol), CuO powder (6.01 mmol), piperidine (15.20 mmol) and HI(aq) (15.20 mmol) were reacted under hydrothermal conditions in an autoclave (Parr Instruments Acid digestion bomb model 276Ac, Teflon lined 304 stainless steel, 45 ml capacity) at 170 °C for 20 h. Colorless crystals were formed that were washed with deionized water and kept at room temperature. The produced compound is stable for months at ambient temperature, pressure and humidity.

2.2. Single crystal diffraction

A single crystal, as judged by appearance, was collected and mounted on a glass fibre with two-component epoxy glue. Since Cu(I)–I systems tend to show some degree of disorder at room temperature due to the mobility of Cu, leading to difficulties in the refinement of the structure, the data collection was performed at 100 K using an Oxford diffraction XCalibur3 system with Mo Kα radiation using a graphite monochromator. Data reduction was performed using the software package CrysAlis RED [5]. The

* Corresponding author. Tel.: +46 8 16 12 58; fax: +46 8 15 21 47.
E-mail address: ehsan.jalilian@mmk.su.se (E. Jalilian).

0025-5408/$ – see front matter © 2011 Elsevier Ltd. All rights reserved.
doi:10.1016/j.materresbull.2011.04.012

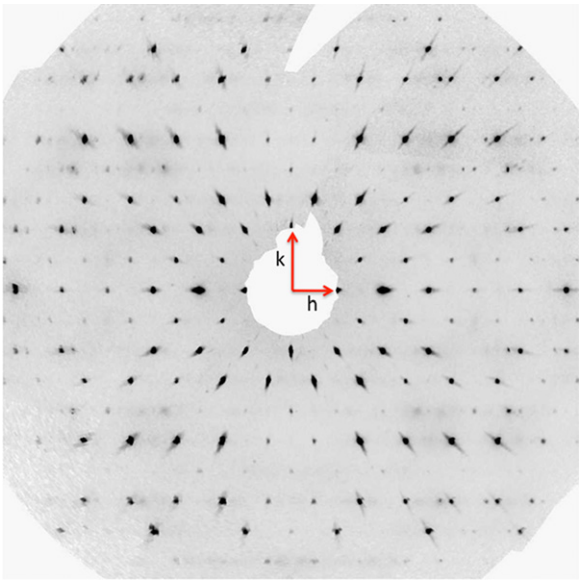

Fig. 1. *h k* 0 plane for the compound presented in this paper.

absorption correction was carried out in the refinement package JANA2000 [6].

2.3. Structure solution

The diffraction pattern displays peculiar non-crystallographic absences that are compatible with twinning. In reciprocal lattice layers perpendicular to the monoclinic *b*-axis, lines of reflections $h = 2n$ display systematic absences corresponding to the reflection condition $h + k = 2n$, i.e. C centering. For lines of reflections $h = 2n + 1$, this condition does not apply. This behavior can be explained by pseudo merohedral twinning that generates a perfect overlap between $h = 2n$ layers, and perfect inter-digitation between $h = 2n + 1$ layers (see Fig. 1).

The structure was solved using Charge Flipping [7] as implanted in the software package Superflip [8], yielding the I, Cu, N and most of the C positions. The structure was refined in a twin model with JANA2000 [6], using the twin matrix [1 0 0; 0 1 0; 1 0 $\bar{1}$] and a fixed 50/50 volume ratio between the twin orientations. Subsequently, remaining C positions were found using difference Fourier analysis. All non-hydrogen positions were refined using full matrix least squares. The hydrogen atoms were located by geometrical methods and refined in a riding model.

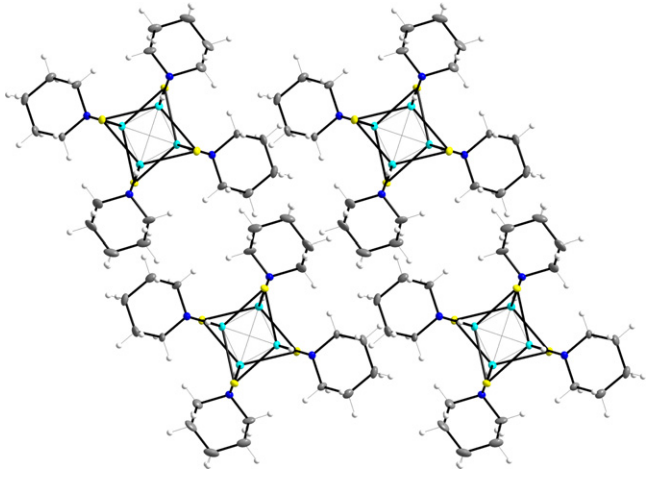

Fig. 2. Packing diagram of the title compound viewed along **b**. I atoms are shown in yellow, Cu in cyan, N blue, C grey and H atoms are white. This color scheme will be used throughout the paper. All non-H atoms are presented by 50% probability ellipsoids. (For interpretation of the references to color in this figure legend, the reader is referred to the web version of the article.)

2.4. Luminescence

Measurement of the emission spectra at ambient temperature and 100 K was carried out using a VARIAN Cary Eclipse Fluorescence spectrophotometer. The emission spectra were collected for different excitation wavelengths, starting at 250 nm and increasing to 360 nm in 10 nm steps.

2.5. Computational details

The calculations were performed using density functional theory with the hybrid B3LYP [9,10] functional as implemented in the Gaussian09 program package [11]. Ground state geometry optimizations with symmetry constraints (C_2 for **A** and D_{2d} for **B**) were carried out using the LANL2DZ basis sets. Analytical frequency calculations were performed to inspect if it is a true minimum (with no imaginary frequencies). For the optical absorption spectrum, the 20 lowest spin-allowed singlet–singlet transitions (C_2 and D_{2d} symmetries) were calculated using TDDFT method. The first symmetry-allowed excited singlet state was optimized using TDDFT method without symmetry constraints. The optimized structure was then used for emission spectrum calculations using the TDDFT method. Isodensity surface plots were constructed using GaussView 4 [11].

3. Results and discussion

The structure crystallizes in the monoclinic crystal system in space group *C*2/*c* with the cell parameters (100 K) $a = 22.653(2)$ Å, $b = 7.6643(2)$ Å, $c = 20.077(2)$ Å and $\beta = 116.557^\circ$ (the cell parameters obtained at room temperature are as follow $a = 22.5791(5)$ Å, $b = 7.7972(4)$ Å, $c = 20.5154(3)$ Å and $\beta = 116.118(4)^\circ$). The structure consists of a tetrahedral (Cu_4I_4) core coordinated by four typical piperidine molecules that are connected via N atom to the Cu atoms giving a total composition $Cu_4I_4(Pip)_4$ (see Fig. 2).

The two modifications of $Cu_4I_4Pip_4$ are very similar. In fact, they are conformational isomers with respect to the Cu coordination of the piperidine N (conf Fig. 3 and Table 1). In the modification reported previously (called **B**), all Cu are equatorial with respect to the piperidine ring, while in the title compound (called **A**) two Cu are equatorial and two are apical. The volume of the monoclinic modification is significantly smaller than that of the tetragonal modification (by a full 6%), and this indicates that it may well be the stable modification.

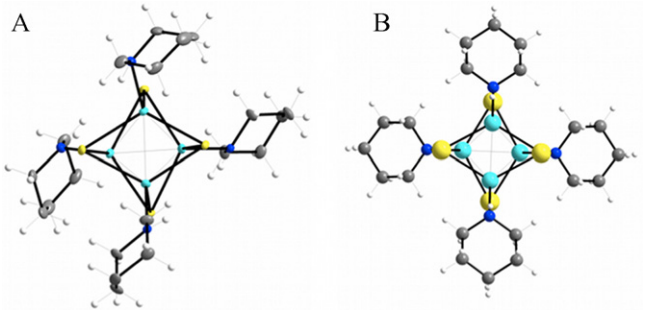

Fig. 3. The Cu4I4 Pip units. **A** shows the unit of the present paper while **B** shows the previously reported unit.

Table 1
Comparison between the crystal presented in this work (**A**) and the previously reported crystal (**B**).[a]

	A (100 K)	**A** (RT)	**B**
Crystal system	Monoclinic	Monoclinic	Tetragonal
Space group	*C*2/*c*	*C*2/*c*	$P4_2/n$
a [Å]	22.6530(18)	22.5791(5)	14.7715(2)
b [Å]	7.6643(2)	7.7972(4)	
c [Å]	20.077(2)	20.5154(3)	7.6073(2)
β [°]	116.557	116.118(4)	90
Density [g/cm^3]	2.348	2.258	2.216
Color	Colorless	Colorless	Colorless/pale yellow
Crystal habit	Flake	Flake	Prismatic

[a]Ref. [4].

The most striking difference between the two modifications is in the luminescent properties. While it is well known that different ligands on the Cu_4I_4 core modify the luminescent properties to a great extent, we believe this is the first reported example where a simple difference in conformation of part of the ligand causes a complete switching between vivid luminescence and none at all. From the emission spectra collected at different excitation wave lengths, it is clear that the most efficient excitation wave length is around 340 nm. The maximum of the emission spectrum is rather broad and appears at 581 nm more or less independent of the excitation wavelength (Fig. 4). To define the nature of the luminescence, whether it is fluorescence or phosphorescence, an attempt to determine the lifetime of the emission was performed resulting in an upper limit of 0.1 ms. This does not conclusively rule out phosphorescence.

To shed more light on why a simple modification can cause this dramatic change in luminescence, we have used quantum chemical methods to calculate both the absorption and emission properties of the two compounds.

3.1. Optimized geometries and electronic structures of the ground states

The crystal structures of **A** and **B** reveal that the complexes adopt geometries that respectively are close to C_2 and D_{2d} point group symmetries. We therefore optimized the ground state geometries under these symmetry constraints. The optimized geometries are shown in Fig. 5 and selected geometric parameters are compared with the X-ray structures in Table 2.

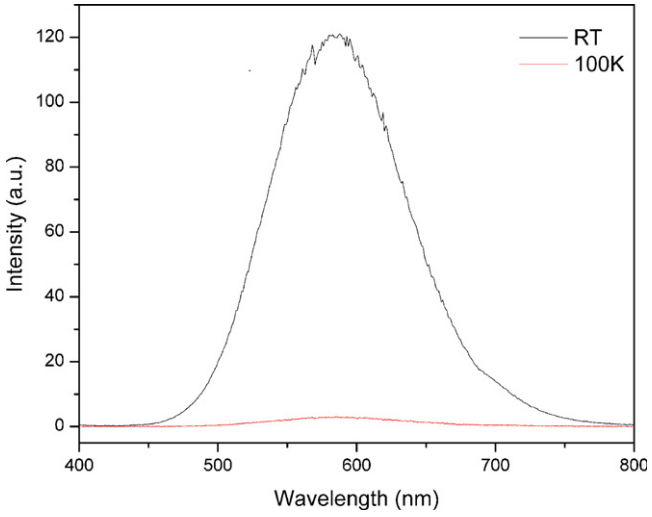

Fig. 4. Emission spectrum for $Cu_4I_4Pip_4$, collected at ambient temperature (black) and 100 K (red). Excitation wavelength is 340 nm and maximum emission is located at 581 nm. (For interpretation of the references to color in this figure legend, the reader is referred to the web version of the article.)

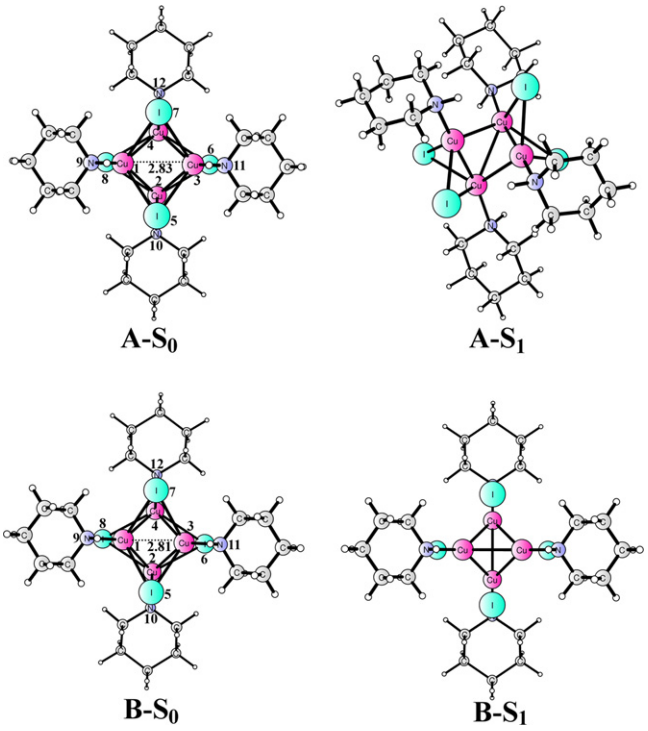

Fig. 5. Optimized structures of the S (C_2 symmetry for **A** and D_{2d} symmetry for **B**) and S1 (no symmetry) states of Cu4I(Pip)$_4$. Distances in angstrom.

Analytical frequency calculations confirm that both **A** in C_2 symmetry and **B** in D_{2d} symmetry have no imaginary frequencies and they are thus true local minima. Compared to the X-ray data, most of the deviations of optimized bond distances in both **A** and **B** are quite small, in general less than 0.2 Å.

It is interesting to note that the calculated energy of **B** is 3.4 kcal/mol lower than that of **A**. Considering that **A** was synthesized under hydrothermal conditions, which should lead to the thermodynamically most stable conformation, the fact that the calculations yield higher energy for **A** compared to **B** (in the case of isolated gas phase compounds) indicates that the crystal packing of **A** must be more beneficial leading to an overall more stable crystal.

Isodensity surface plots of three important molecular orbitals (HOMO-1, HOMO, and LUMO) of both **A** and **B** are shown in Fig. 6. The nature of these three MOs are very similar for **A** and **B**. The

Table 2
Optimized geometric parameters of $Cu_4I_4(Pip)_4$ in the S0 and S1 states, with comparison to the X-ray structure data (distance in angstrom).

	A (C_2 symmetry)			**B** (D_{2d} symmetry)		
	X-ray	S0	S1	X-ray	S0	S1
Cu_1–Cu_2	2.64	2.71	2.66	2.67	2.69	2.53
Cu_1–Cu_3	2.60	2.83	2.42	2.63	2.81	2.67
Cu_1–Cu_4	2.62	2.71	2.77	2.67	2.69	2.53
Cu_2–Cu_3	2.62	2.71	2.85	2.67	2.69	2.53
Cu_2–Cu_4	2.76	3.12	2.42	2.63	2.81	2.67
Cu_3–Cu_4	2.62	2.71	2.67	2.67	2.69	2.53
Cu_1–I_5	2.70	2.86	2.91	2.69	2.86	3.06
Cu_2–I_5	2.66	2.76	3.72	2.70	2.80	3.04
Cu_2–I_6	2.71	2.92	2.81	2.72	2.86	3.06
Cu_3–I_5	2.67	2.86	2.83	2.72	2.86	3.06
Cu_1–N_9	2.05	2.10	2.06	2.05	2.10	2.05

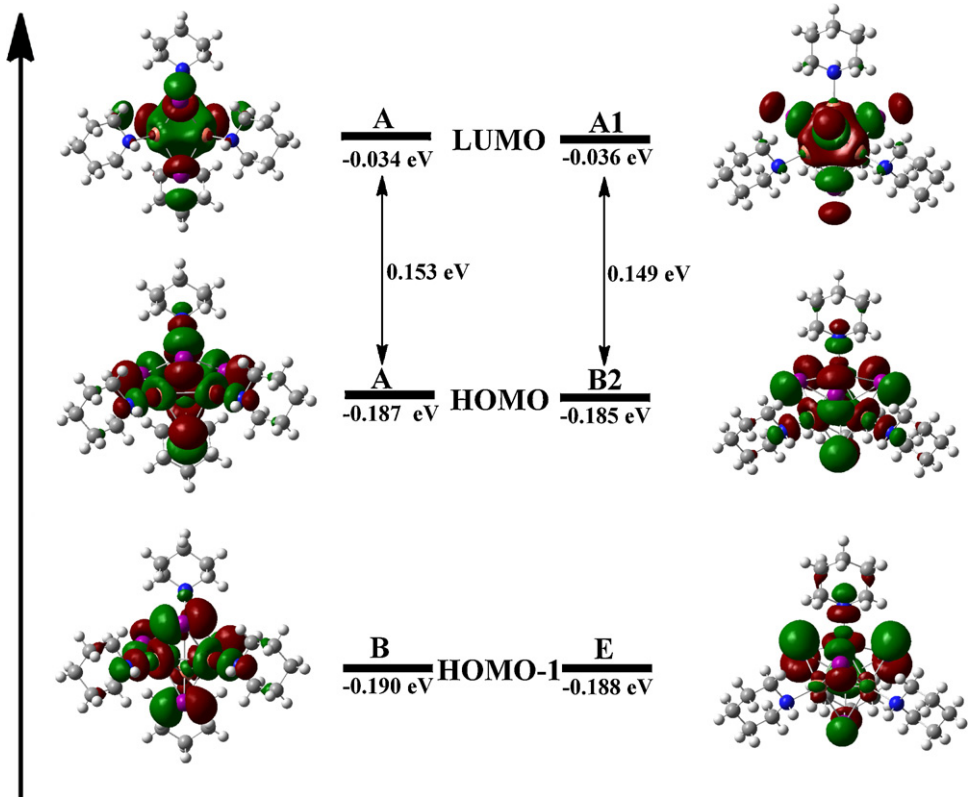

Fig. 6. Energy levels and isodensity surface plots of selected orbitals for the ground states of **A** (C_2, left) and **B** (D_{2d}, right).

LUMO has a bonding character of the tetrahedral Cu_4 center and an anti-bonding character of the Cu–I bonds. These features are quite similar to those calculated previously for the $[Cu_4I_4(pyridine)_4]$ and $[Cu_4I_6]^{2-}$ complexes [12–15]. For **A**, both the HOMO and the LUMO belong A symmetry, and thus the HOMO–LUMO excitation will be symmetry-allowed. For **B**, the HOMO and the LUMO belong to B2 and A1 symmetries, respectively, showing that also here the HOMO–LUMO excitation is symmetry-allowed.

3.2. Optical absorption spectrum

TDDFT calculations were performed to obtain the 20 lowest excited singlet states for both **A** and **B** (the 10 lowest are listed in Table 3). The absorption spectrum of **A** was first calculated using the X-ray structure, i.e. without performing geometry optimization. The lowest excited state, corresponding to a HOMO–LUMO excitation (Table 4), has an absorption wavelength of 333 nm, with a quite weak intensity (oscillator strength (f) of 0.0004). This wavelength agrees quite well with the experimental results which showed that the best excitation wavelength is at 340 nm. Geometry optimization of **A** leads overall to longer absorption wavelengths, by ca. 40 nm.

Very similar results were obtained for compound **B** (see Table 3), which indicates that the two modification should have similar absorption properties.

3.3. Singlet excited states: emission

To obtain the emission properties, we have considered the de-excitation from the lowest excited singlet state (S1) of the two modifications. Geometry optimization of the S1 states was performed using TDDFT starting from the ground state structures for both **A** and **B** without any symmetry constraints. The optimized structures are shown in Fig. 5.

Table 3
Calculated TDDFT singlet–singlet excitation wavelengths (λ, nm) and oscillator strengths (f) of $Cu_4I_4(Pip)_4$.

Excited state	**A**					**B**				
	X-ray		Optimized (C_2)			X-ray		Optimized (D_{2d})		
	λ	f	Symmetry	λ	f	λ	f	Symmetry	λ	f
1	333.0	0.0004	A	374.5	0.0008	333.9	0.0031	B2	384.6	0.0010
2	326.7	0.0017	B	364.9	0.0013	330.7	0.0019	E	375.6	0.0007
3	324.2	0.0032	B	364.8	0.0023	330.7	0.0019	E	375.6	0.0007
4	294.8	0.0081	A	340.5	0.0	298.1	0.0156	A2	347.9	0.0
5	292.4	0.0482	B	327.7	0.0323	298.1	0.0156	E	339.9	0.0070
6	292.4	0.0872	A	327.5	0.0762	296.4	0.0864	E	339.9	0.0070
7	290.9	0.0365	B	325.1	0.0442	294.2	0.0	B2	335.0	0.0795
8	290.0	0.0027	B	324.4	0.0459	293.3	0.0748	E	333.5	0.0741
9	286.7	0.0835	B	318.6	0.0336	293.3	0.0748	E	333.5	0.0740
10	280.2	0.0144	A	300.0	0.0	276.2	0.0273	A2	305.7	0.0

Table 4
Composition of main orbital singlet–singlet transitions of $Cu_4I_4(Pip)_4$. Only main transitions with largest coefficients are given.

Excited state	**A**		**B**	
	X-ray	Optimized (C_2)	X-ray	Optimized (D_{2d})
1	HOMO → LUMO	HOMO → LUMO	HOMO → LUMO	HOMO → LUMO
2	HOMO-1 → LUMO	HOMO-1 → LUMO	HOMO-1 → LUMO	HOMO-1 → LUMO
3	HOMO-2 → LUMO	HOMO-2 → LUMO	HOMO-2 → LUMO	HOMO-2 → LUMO
4	HOMO-6 → LUMO	HOMO-5 → LUMO	HOMO-6 → LUMO	HOMO-6 → LUMO
5	HOMO-4 → LUMO	HOMO-3 → LUMO	HOMO-7 → LUMO	HOMO-8 → LUMO
6	HOMO-3 → LUMO	HOMO-4 → LUMO	HOMO-3 → LUMO	HOMO-7 → LUMO

Since the LUMO orbitals of both **A** and **B** have a bonding character of the cubic Cu_4 core and an anti-bonding character of the Cu–I bonds, the excitation from HOMO to LUMO induces contraction of the cubic center and elongation of the Cu–I distances. However, the two modifications have very different S1 geometries, as seen in Fig. 5.

While the S1 geometry of **B** maintains its symmetric cubic core, albeit with shorter Cu–Cu distances and longer Cu–I distances, **A** relaxes more into a structure where the iodides coordinate to two copper atoms each (see Fig. 5).

For **A**, the energy of the optimized S1 state is 2.28 eV higher than that of the optimized S_0 state. For **B**, the corresponding value is 2.69 eV. These energies results in emission wavelength of 782 nm for **A** (oscillator strength 0.002) and 566 nm (oscillator strength 0.011) for **B**. These values should be compared to the experimental emission wavelength observed for **A**, which has a maximum peak at 581 nm.

Clearly, the geometry of the S1 state of **A** has in the optimization relaxed too much, which could be a result of the fact that the optimization was performed for the isolated compound, i.e. without the surrounding crystal. It is possible that the crystal packing of **A** is such that it prevents such a relaxation. The experimental crystal densities of the two modifications seem to be consistent with this conclusion. While **B** has a density of 2.216 g/cm^3, **A** is about 2% more dense (ρ = 2.258 g/cm^3).

These results indicate thus that although the absorption properties of the two modifications are very similar, the emission properties differ a lot. A possible reason for this could be the crystal packing which influences the geometry of the S1 state.

4. Conclusions

We have in this paper presented synthesis of a new modification of the $Cu_4I_4Pip_4$ crystal, which, in contrast to previous reports, is luminescent. We have solved the crystal structure and measured both the absorption and emission spectra. In addition, we have performed quantum chemical calculations to characterize the properties of the two modifications. Based on these calculations, we speculate that the crystal packing could influence the fluorescence of the compounds.

Acknowledgment

Professor emeritus Bertil Forslund at Stockholm University, Department of Materials and Environmental chemistry is acknowledge for his help with fluorescence spectrophotometer.

Appendix A. Supplementary data

Supplementary data associated with this article can be found, in the online version, at doi:10.1016/j.materresbull.2011.04.012.

References

[1] E. Jalilian, S. Lidin, Acta Crystall. Sect. C 0108-2701 66 (2010) m227.
[2] M. Vitale, P.C. Ford, Coord. Chem. Rev. 219 (2001) 3.
[3] P.C. Ford, E. Cariati, Bourassa, J. Chem. Rev. 99 (1999) 3625.
[4] V. Schramm, Inorg. Chem. 17 (1978) 714.
[5] CrysAlis CCD Data Reduction, 1.171.32.24 ed., Oxford Diffraction Ltd., Yanton, England, 2008.
[6] V. Petricek, M. Dusek, L. Palatinus, Jana2000. The crystallographic computing system, Institute of Physics, Praha, Czech Republic, 2000.
[7] G. Oszlanyi, A. Suto, Acta Crystall. Sect. B-Struct. Sci. A 60 (2004) 134.
[8] L. Palatinus, G. Chapuis, J. Appl. Cryst. 40 (2007) 786–790.
[9] A.D. Becke, J. Chem. Phys. 98 (1993) 5648.
[10] C.T. Lee, W.T. Yang, R.G. Parr, Phys. Rev. B 37 (1988) 785.
[11] G.W. Frisch, et al., Gaussian 09, Revision A.1, Gaussian, Inc., Wallingford, CT, 2009
[12] M. Vitale, W.E. Palke, P.C. Ford, J. Phys. Chem. 96 (1992) 8329.
[13] M. Vitale, C.K. Rye, W.E. Palke, P.C. Ford, Inorg. Chem. 33 (1994) 561.
[14] F. De Angelis, S. Fantacci, A. Sgamellotti, E. Cariati, R. Ugo, P.C. Ford, Inorg. Chem. 45 (2006) 10576.
[15] E. Jalilian, R.-Z. Liao, F. Himo, H. Brismar, F. Laurell, S. Lidin, CrystEngComm, in press.